Development 120, 265-276 (1994)
Printed in Great Britain © The Company of Biologists Limited 1994



# Cell cycles and clonal strings during formation of the zebrafish central nervous system

**Charles B. Kimmel*, Rachel M. Warga† and Donald A. Kane†**

Institute of Neuroscience, University of Oregon, Eugene, Oregon, 97403, USA

*Author for correspondence
†Present address: Max Planck Institut fur Entwicklungsbiologie, Spemannstrasse 35, D7400, Tübingen, Germany

## SUMMARY

**Cell lineage analysis of central nervous system progenitors during gastrulation and early segmentation in the zebrafish reveals consistent coupling of specific morphogenetic behaviors with particular cell cycles. Cells in single clones divide very synchronously. Cell divisions become progressively oriented, and act synergistically with oriented intercalations during the interphases of zygotic cell cycles 15 and 16 to extend a single lineage into a long, discontinuous string of cells aligned with the nascent embryonic axis. Dorsalwards convergence brings the string to the midline and, once there, cells enter division 16. This division, or sometimes the next one, and the following cell movement reorient to separate siblings across the midline. This change converts the single string into a bilateral pair of strings, one forming a part of each side of the neural tube. The stereotyped cellular behaviors appear to account for the previously reported clonal restriction in cell fate and to underlie morphogenesis of a midline organ of proper length and bilateral shape. Regulation of cellular morphogenesis could be cell-cycle dependent.**

Key words: cell lineage, convergence, extension, cell cycle, axial development, neurulation

## INTRODUCTION

We would like to learn how clones of cells develop and participate in forming the body of a vertebrate, and whether cell lineage plays a significant role in establishing body pattern and specifying cell fate. Cells might inherit instructions about how to develop from their parents, and lineage analysis explores this pathway of information flow, as well as serving as a powerful way to examine cellular behaviors during normal development.

In the zebrafish, blastula cells intermix extensively as the blastoderm thins during epiboly, the embryo's first morphogenetic movement (review: Wilson et al., 1993). As gastrulation begins, single cells frequently give rise to restricted clones of progeny (Kimmel and Warga, 1986; Kimmel et al., 1990). In such clones, every descendent cell develops the same tissue- or organ-specific fate, although not necessarily the same cell-specific one. Moreover, the pattern of distribution of the lineally related cells within the tissue that they make can be highly stereotyped. For example, cells of a single clone restricted to the central nervous system (CNS) become arranged within the neural tube as a bilateral pair of discontinuous lines. In this paper, we refer to these clonal arrays as 'strings', to emphasize that they are long and narrow, sometimes not wider than a single cell. The strings are oriented along the neuraxis and the cells can be distributed periodically within them (Kimmel and Warga, 1986). Such striking cell distributions indicate that both the cell divisions that expand a clone and the cell rearrangements that shape it (Keller et al., 1992a; Warga and Kimmel, 1990) are under strict control. The control could begin as early as the midblastula transition, when zygotic transcription is first detected (Kane and Kimmel, 1993). At this stage, three mitotic domains of cells arise, each of them playing a separate role during epiboly (Kane et al., 1992). The correlation between cell cycle behavior and morphogenesis might indicate the two processes are coordinately regulated, that is, somehow controlled together, or interdependently.

The formation of clonal strings that occurs later during organogenesis in one of these domains clearly involves highly ordered cell intercalations (Warga and Kimmel, 1990) that drive the convergence and extension movements shaping the organ primordia (Keller and Tibbetts, 1989; Keller et al., 1989; 1991; 1992b). Oriented cell divisions could be involved as well, as suggested from serial section analysis of avian neural tube formation (Schoenwolf and Avarez, 1989; see also Schoenwolf and Smith, 1990).

In this paper, we examine directly the relationships between cell cycles and cellular morphogenetic behavior in single neural lineages. We follow the cells as tissue restrictions first arise, during convergence and extension, and, in some cases, until after young neurons are postmitotic. Remarkably, cells in single clones all tend to divide together through the period of gastrulation, and they all tend to orient their divisions and intercalations, and hence their movements, the same way at particular cell cycles. Cells separate *along* the anterior-posterior

(AP) axis during two cell cycles, generating clonal strings. The second one of these cycles is the last one for some neurons. The division that ends it occurs at the embryonic midline, and this division separates sisters *across* the AP axis to produce the bilateral string pairs. Hence, specific cell movements are coupled to specific cell cycles in the gastrula and afterwards, suggesting that morphogenesis might be regulated in a cell-cycle-dependent manner.

## MATERIALS AND METHODS

### Embryos and lineage tracer injections

Zebrafish, *Danio (Brachydanio) rerio*, embryos came from natural spawnings of laboratory strains, usually bearing the *golden*$^{b1}$ pigment-pattern mutation (Streisinger et al., 1986), which lightens melanocytes and facilitates viewing the clones in whole-mounted live embryos at advanced stages. We staged the embryos by morphology (Warga and Kimmel, 1990), which permits accurate determination of the cell number, and hence zygotic cell cycle number, through the eleventh cleavage, about 3.3 hours after fertilization (ending cycle 11; see Kane and Kimmel, 1993). Times are expressed as hours postfertilization at 28.5°C (h). Injections of lineage tracer, rhodamine-dextran, were made into single blastomeres (Warga and Kimmel, 1990), and examined immediately afterward by fluorescence to ensure that only one cell was labeled.

Most injections were at latitudes in the blastoderm that generate neural fates and fairly close to the blastoderm margin (for examples, see Fig. 3 in Kimmel et al., 1990). Such placements tend to select against lineages that form the anterior parts of brain and which would be relatively difficult to analyze because of formation the CNS flexures and the greater diameter of the anterior brain. Accordingly, most clones that we studied populate the spinal cord, and extend anteriorly into the hindbrain, occasionally the midbrain.

### Time-lapse microscopy

Embryos were mounted for recording between coverslips in agar as described by Warga and Kimmel (1990). Images were made using a Zeiss Universal or UEM microscope, with UV epi-illumination (including neutral density filters in the light path to minimize damage to the labeled cells) and equipped with a Dage low light (Silicon Intensified Target) video camera. Most of the recordings were made using a 16× objective. In our earlier experiments, recordings were stored on video tape (Gyre recorder) and in later ones on optical memory disk (Panasonic model no. 3040 Optical Memory Disc Recorder). The microscope was equipped with a motor driven focus controller and motor driven shutters for the both white light and UV sources. An Apple Macintosh II Computer, equipped with Quickcapture digitizing board and a RasterOps auxiliary monitor, with Neurovideo software (Myers and Bastiani, 1991; a current version now available as 'Axovideo', from Axon Instruments) was used for controlling the shutters, focus and time-lapse parameters and for image enhancement. To improve resolution of the low light images, for each time and depth we digitized and averaged 3-10 images from the SIT camera, and then recorded the resulting processed image on the OMDR. Generally we stored both UV and white light images at 5 depths of focus (intervals of 10-30 μm) and at time intervals ranging from 1.5 minutes(during early epiboly, when cells divide and move rapidly) to 5 minutes (during segmentation, when divisions and movements occur much more slowly). Recordings were continued for 8-24 hours, and the embryos inspected occasionally thereafter, for up to 3 days of development.

## RESULTS

### Cell arrangement in CNS clones is stereotyped

We examine clones in the embryonic brain and spinal cord that derive from single dye-filled blastula progenitors (Fig. 1). There are two very consistent features of cell arrangement in such clones, as has been described previously (Kimmel and Warga, 1986). First, the clones always extend markedly in the anterior-posterior (AP) direction. Labeled cells are invariably present among unlabeled ones, either dispersed singly or into clusters. The degree of AP extension of the entire clone can vary substantially, as the particular examples that we selected in Fig. 1 illustrate. Clones within the spinal cord are more extended, and their cells more dispersed, than those within the brain.

Second, labeled cells always occupy both sides of the CNS. For every clone, but not invariably for every cell in a clone, one is impressed that the cells lie in a mirror-image symmetrical pattern across the midline. Clone N4 presents a particularly striking bilateral arrangement. Sometimes, opposing labeled cells are bilateral homologues (c motoneurons in clone N5). Other times, similar but not identical cells lie opposite one another (c and CaP motoneurons in N6). Occasionally a labeled cell or cell cluster has no contralateral counterpart (e.g. a right-side cluster at the level of somite 1 in clone N6).

We only observe clones with bilateral arrays of labeled cells in the CNS. Clones contributing to other axial organ systems are AP-extended, but in the head and trunk are restricted to only one side of the midline (e.g. for somitic muscle see Kimmel and Warga, 1987).

### The cell cycle of origin of CNS-restricted progenitors is variable

Cell lineage analysis, by video time-lapse recording in vivo, reveals when cells contributing to the CNS originate and how they develop subsequently (Fig. 2). The records begin with a single dye-labeled cell in the blastula enveloping layer (EVL), and in a cell cycle ranging between zygotic cycle 10 and 12 (see Kane and Kimmel, 1993). The EVL will not itself form CNS, but persists through embryogenesis as an outermost simple epithelial covering of the embryo (the periderm). Neural progenitors arise in the deep cell domain, located beneath the EVL. Until the late blastula period EVL cells contribute to the deep cell domain during mitoses. In the examples in Fig. 2, the first division of the injected EVL cell (or the second division in clones N3 and N7) yields a deep cell. The sister of this deep cell remains in the EVL and typically generates an EVL-restricted sublineage. Most restrictions to the EVL occur by division 11 (the division completing cycle 11; 12 out of 15 cases). The last of them occur in the late blastula at division 12 (clones P, M, N5).

In some embryos, the first deep cell arising from the EVL progenitor generates a sublineage restricted to the CNS (e.g. N1-N3; Fig. 2) or another embryonic tissue (P, M). In other cases, a subsequent deep cell division segregates CNS and non-neuronal sublineages (e.g. N4). As for the EVL restriction, the cycle that generates CNS-restricted deep cells varies among embryos and among deep cell sublineages within a single embryo. For example, compare the two sublineages in clone N7 (Fig. 2). In the more anterior one (to the left in the figure), a neural-restricted deep cell segregates from the EVL at division 11. However, the posterior-most deep cell in clone N7 (the right-most in Fig. 2) remains unrestricted until division 14. This division, occurring just at gastrulation onset (arrow), segregates neural and muscle fates.

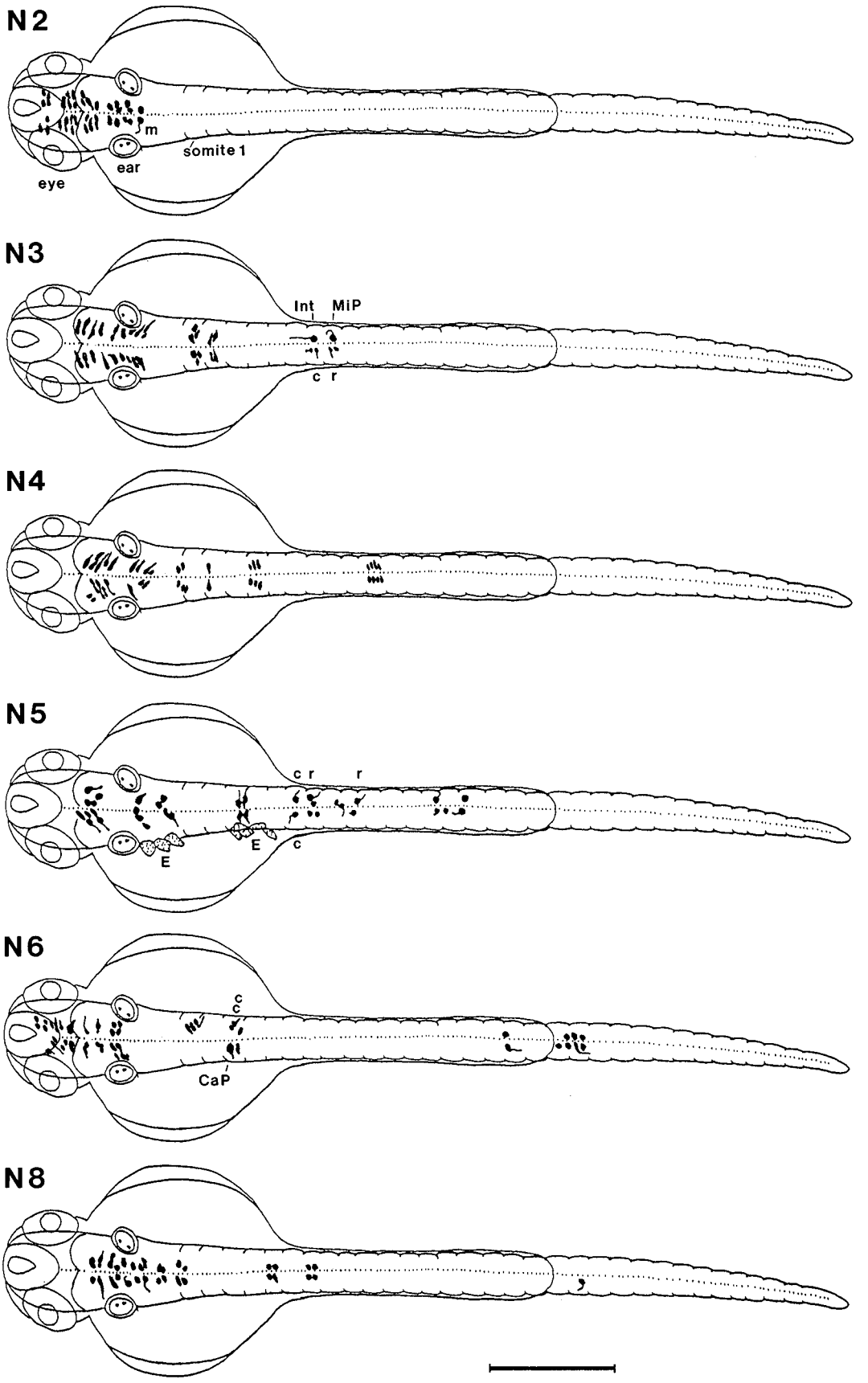


**Fig. 1.** CNS clones form bilateral cell clusters dispersed along the neuraxis. Dorsal views with anterior to left of clones (N2-N8) selected to encompass the range in AP-extension. The lineages that generated these clones are included in Fig. 2, where the embryo designations correspond. The positions of dye-labeled cells in live embryos at about 24 h were recorded on an optical disk, and later sketched on a template, from which these drawings were made. Sometimes details were added from inspections of the same clone at later stages (e.g. the identity of a neuron whose axon had not yet grown at 24 h). The clones all begin anteriorly in the hindbrain, or the midbrain (N2, N6), and vary markedly in how far they extend posteriorly; N2 ends in the sixth hindbrain rhombomere, and N6 and N8 have one or more cells in the tail spinal cord. Notice that clusters in the brain are more compactly distributed and contain more labeled cells than those in the spinal cord. The clones include many neurons, whose types we could ascertain by examining the course of their dye-filled axons. A few, corresponding to cells discussed further below (Table 2, Fig. 7) are indicated. Cell m (N2) is a motoneuron contributing to cranial nerve IV. Int is a ventral spinal interneuron with an ascending axon. MiP and CaP are primary spinal motoneurons; c and r are secondary spinal motoneurons (defined in the legend to Fig. 7). Many other cells in the clones are not postmitotic at 24 h, but will continue to divide. For N5 the entire clone deriving from the injected enveloping layer blastomere (see text) is shown. The enveloping layer descendants (E) are stippled. All of the other clones included the enveloping layer, and N4 and N8 also contained labeled mesoderm (See Fig. 2). These cells are omitted here for the sake of clarity. Scale bar, 200 μm.

### Clonally related deep cells divide synchronously during gastrulation

Irrespective of when restrictions arise, or of eventual fate, deep cells in single clones tend to divide very synchronously, often within a few minutes of one another (Fig. 2). They maintain synchrony through the end of gastrulation, when they are in cycle 16. The EVL cells, in a separate mitotic domain (Kane et al., 1992), divide less rhythmically, and also less rapidly.

Deep cell cycles lengthen progressively (Table 1), and lengthen similarly in nearly all of the clones. Cycles 15 and 16 are longer than usual in clone N10, and particularly long in clone N11 (Fig. 2). Both clones were located on the ventral side of the developing gastrula and later contribute to the tail. In contrast, all of the other clones were dorsal or dorsolateral and contribute mostly to the head and trunk (examples in Fig. 1). Interestingly, lineage restrictions of deep cells also occur later in clones N10 and N11 than in any of the others (Fig. 2). These findings might mean that both deep cell cycle lengths and onsets of lineage restrictions vary according to dorsoventral blastoderm position. However, one would need to examine more examples of ventral clones to learn if such a correlation is really present.

### Clonal strings arise by oriented intercalations and cell divisions in the late gastrula

The time-lapse records clearly show how the developing clones undergo the morphogenetic movements of epiboly, convergence and extension. Epiboly spreads all of the cells, including EVL cells, in a posterior direction, but only deep cells undergo marked convergence and extension (Fig. 3). Convergence sweeps the deep cells towards the dorsal midline, producing a drift of them away from their EVL relatives (Fig. 3E) and ends during cycle 16 (Fig. 3F). Extension is evident as the deep cells separate from one another, beginning in the early gastrula (Fig. 3C,D). The cells form a discontinuous AP-oriented string

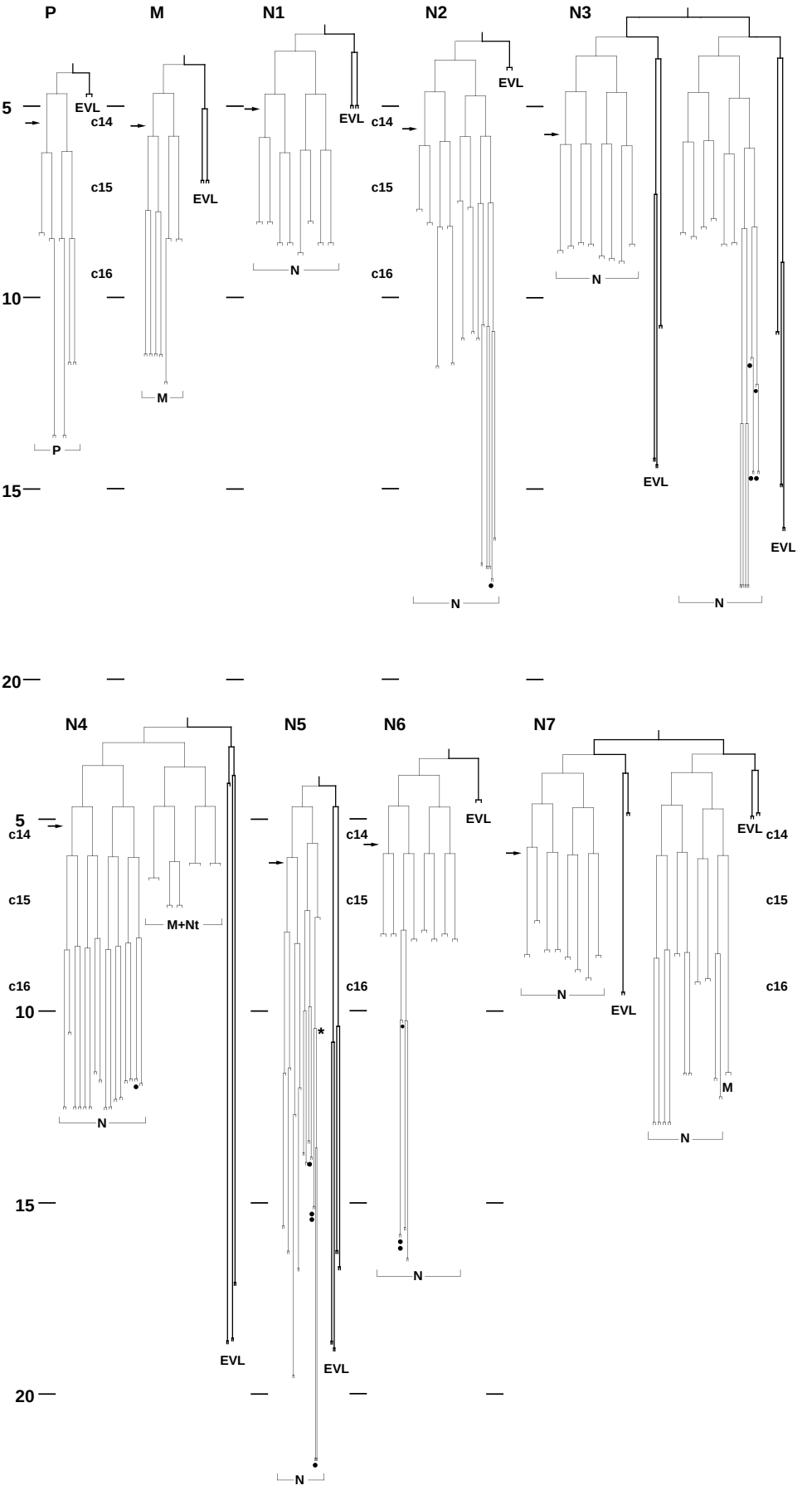

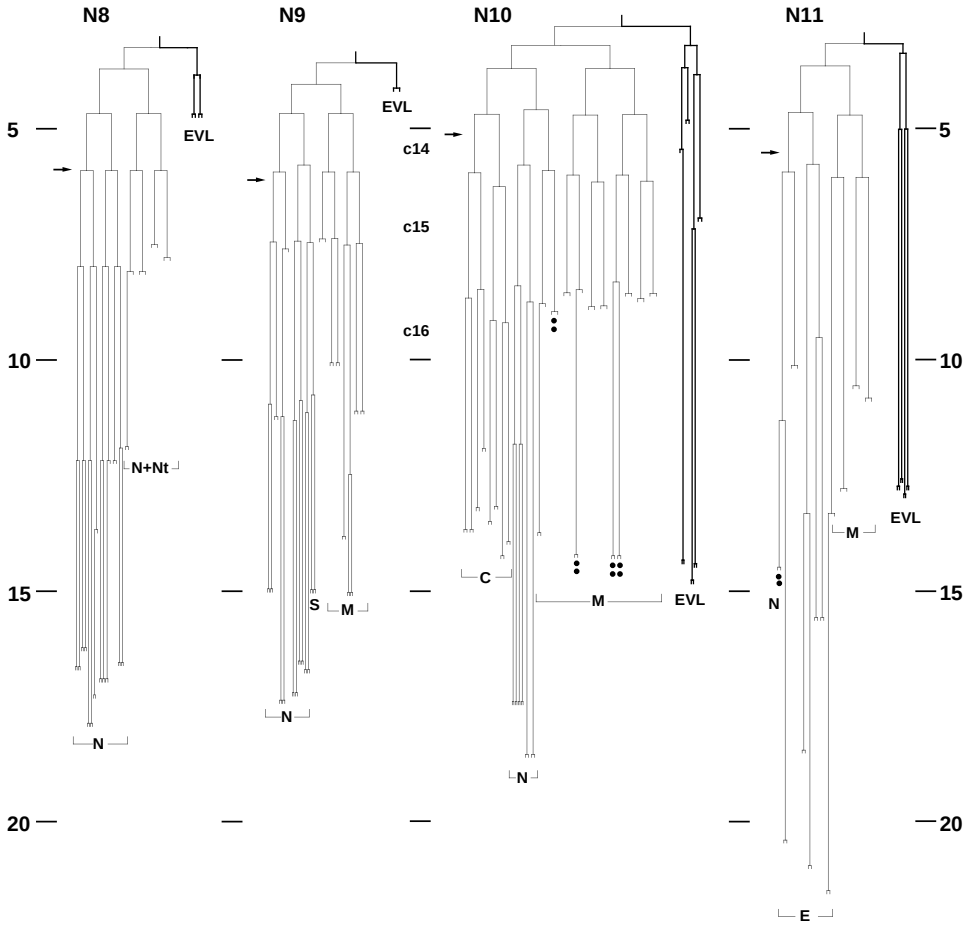


**Fig. 2.** Cell lineage analysis reveals segregation patterns and division synchrony among deep cells during gastrulation. The vertical scale shows hours postfertilization (h). Gastrulation begins between 5 and 6 h, and segmentation (somite formation) begins at about 10 h. Cell cycle numbers (c14, c15, c16) are defined by the fertilized egg starting cycle 1, with division 1 occurring at the end of cycle 1. The lineages begin with a single dye-injected enveloping layer (EVL) blastula cell present at 3-4 h and show all of the divisions that we could assign from video time-lapse recordings of the clones. A branch ending on the diagram means that we did not record further divisions along it, even though we may have followed the cells for several hours after the branch ends. In some cases, indicated by dots at the ends of the lines, the cells differentiated, showing that they were postmitotic (Table 2; Fig. 7). More often, the cells continued to divide after the recording session, and had formed clusters when they were reinspected later (e.g. Fig. 1). The first or second divisions segregate EVL-restricted lineages, shown as unlabeled heavy lines branching to the right. The thin lines branching to the left represent lineages of deep cells. They are labeled at their ends according to tissues that they made. The deep sublineages in clones P and M were respectively restricted to pharyngeal endoderm (P) and trunk muscle (M). The other clones all made neural tissues (N), and are ranked N1-N11 according to the AP position of the middle of the clone, as measured from the anterior end of the embryo at 24 h. A clone of small rank (N1) is more anterior and generally more compact than one of large rank. Some of these clones included other tissue types, neural crest (C), epidermis (E), notochord (Nt) and somite epithelium (S, an epithelial surrounding layer that may be distinct from the myotome). For deep cell divisions earlier than cycle 16, the branches to the left represent the more anterior sisters. Thus, in clone N4, the anterior deep cell sublineage arising at division 11 contributed to the CNS, and the posterior sublineage contributed to two tissues, muscle and notochord. All of the other figures in the paper are oriented in the same fashion. The horizontal arrows along the diagrams indicate the time we estimated each embryo to have reached the 50%-epiboly stage, when gastrulation begins (Warga and Kimmel, 1990). However, we could not determine this stage very accurately with embryos mounted for recording, and these diagrams are vertically aligned by assuming that division 13 occurs at 4.7 h (late blastula stage). In fact there is variability in the time of this division (Kane and Kimmel, 1993). Hence, while this figure shows that blastula and gastrula deep cell cycles are similar in length from embryo to embryo, one cannot assume that the divisions are occurring synchronously between embryos. We also do not know whether, in a single embryo, the divisions of unlabeled cells near the clone occur during the same wave.

by the beginning of cycle 16 (Fig. 3E), and the string still rapidly lengthens after its convergence is over (Fig. 3G).

We observed an AP-oriented cell string to emerge during cycles 15 and 16 in every clone that we followed. Differences in the final degree of AP extension among clones (Fig. 1) are due to different rates of cell separations during cycles 15 and 16, particularly during cycle 16 (Fig. 4). The rate of separation, in turn, reflects how fast the labeled cells are mixing among unlabeled neighbors. Intercalations can separate adjacent cells along the string by 1-2 cell diameters (clone N2) or by of as many as 5 cell diameters (N4). In some clones (N2, N8), all of the cells separate by approximately the same spacing and, in others (N4), adjacent cousins separate farther than sisters. The cells separate at rather constant rates during the interphases of cycles 15 and 16, most rapidly during cycle 16; the overall curves approximate exponentials (inset, Fig. 4). Extension occurs because the cell intercalations are oriented preferentially in the mediolateral direction (Keller et al., 1989). Mediolateral intercalation is well illustrated by following the behavior of the black and white cells in the middle of the N8 string (Fig. 4; also see Warga and Kimmel, 1990).

As apparently occurs in avian embryos (Schoenwolf and Alverez; 1989), the neural progenitors in zebrafish orient not only their intercalations but also their divisions. Division 15 frequently separates sister pairs along the AP axis (Fig. 5A-C). This is the same direction in which the cells continue to separate, because of intercalations, after division 15. Division 14, occurring in the early gastrula, seems not so strongly oriented (Fig. 6). The one before that, division 13 in the blastula, may be occurring randomly relative to the AP axis. However, all of these divisions, irrespective of cycle numbers, were oriented to produce sister pairs at the same depth in the blastoderm; i.e. the divisions were tangential rather than radial.

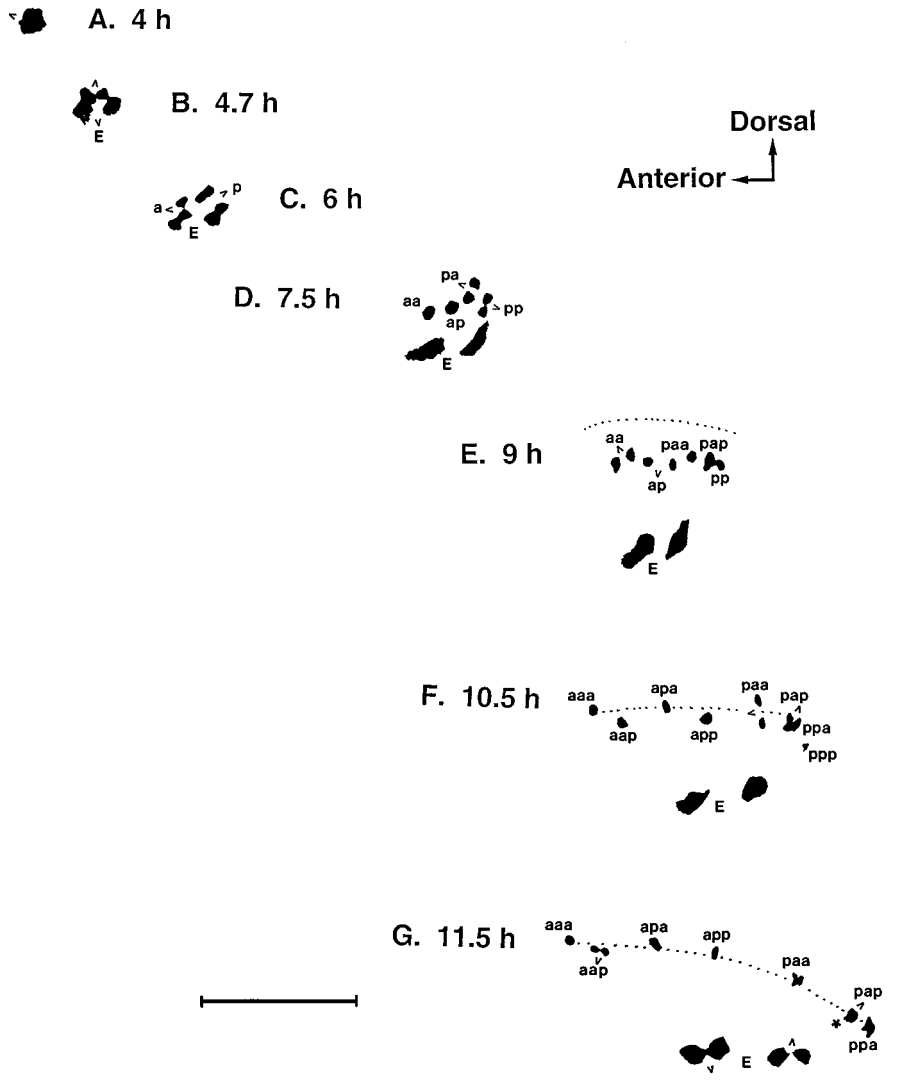


**Fig. 3.** An expanding clone of cells undergoes morphogenetic rearrangement to form a string during gastrulation. Sample views of the clone N5 during late blastula (A,B), gastrula (C-E), and early segmentation (F,G) stages, selected to show the positions of cells generally not long after cell divisions (v) occurred. The figure is reproduced from negative processed video images of our time-lapse series of records, such that the fluorescent cells here appear black on a white background. Time increases down the page. Intercalations did not substantially mix up the order of the deep cells in this clone such that the left-most cell in this figure corresponds to the left-most branch in the lineage diagram for clone N5 in Fig. 2. The set of single deep cells at 11.5 h (G) corresponds in a 1:1 fashion to the bilateral set of cell clusters present at 24 h (Fig. 1, N5). The first division of the injected cell, division 12, generates an EVL-deep sister pair (A). Cells in the EVL sublineage (labeled E at each time point) look larger because they are flattened. The EVL cells divide only twice (B and G). For the deep cells, division 13 occurs at B to generate anterior (a) and posterior (p) daughter cells, both cell a and p complete division 14 at C. Division 15 is completed in the p sublineage at D and in the a sublineage in E. Some of the cells are in division 16 at F and G. The star (G) indicates a particular division 16 that is generating the mother cell of a pair of type c motoneurons, and the grandmother cell of a type r motoneuron. A star appears at the corresponding place along the lineage diagrams for N5 in Figs. 2 and 7. Epiboly produces the drift to the right side of the figure (posterior in the embryo). Convergence of deep cells separates them from their EVL relatives, beginning at about 6 h (C), and is over at 9 h (E). The separation occurs in an upwards direction in this figure, towards the dorsal midline in the embryo; this clone originates from a left-side dorsolateral position in the blastoderm. Extension produces the deep cell string evident at 9 h (E), and elongates it thereafter. One cell at the posterior end of the string is missing at the last time point (cell ppp in G) because it moved out of the field being recorded. Scale bar: 200 μm.

Not every cell divides, or moves, as the majority do, and the relation between division and movement orientation is not strict. The daughters of the two cells dividing in an apparently 'wrong' way at division 14 in clone N5 (Fig. 6) rapidly made an AP-oriented string during cycle 15 in spite of this (Fig. 3).

We presume, but have not directly demonstrated, that orientation of division plane depends on the orientation of the mitosis.

### Strings split bilaterally at division 16

As the cells in CNS clones converge dorsomedially, they are in cycle 16, at least at hindbrain and trunk spinal cord levels that we have studied. The string of cells reaches the dorsal midline and convergence ends. While the cells are positioned just at the midline they divide, and do so with a new orientation. This division, division 16, frequently occurs roughly in the sagittal plane, separating the sister cells across the midline (Figs 5D-F, 6). During the interphase following this division, one of the sisters often continues to move to the left and the other one continues to the right, which produces a bilaterally symmetrical pattern (Fig. 4, clones N2 and N8). We never observed a midline separation earlier than division 16, but we observed a few that were later. For example, in clone N5, bilateral sister motoneurons separated as postmitotic cells after their birthday division 17 (the c pair in Fig. 1). Such separations might not occur after division 18. By this stage, the solid neural keel that is characteristic of early teleost embryos

**Table 1. Cell cycle lengths increase progressively during gastrulation**

| Cycle number | No.* | Length (minutes) mean ± s. d. |
|---|---|---|
| 13 | 26 | 54±9 |
| 14 | 60 | 78±8 |
| 15 | 118 | 151±59 |
| 16 | 91 | 240±71 |

*Number of complete deep cell cycles recorded in clones in 14 embryos.

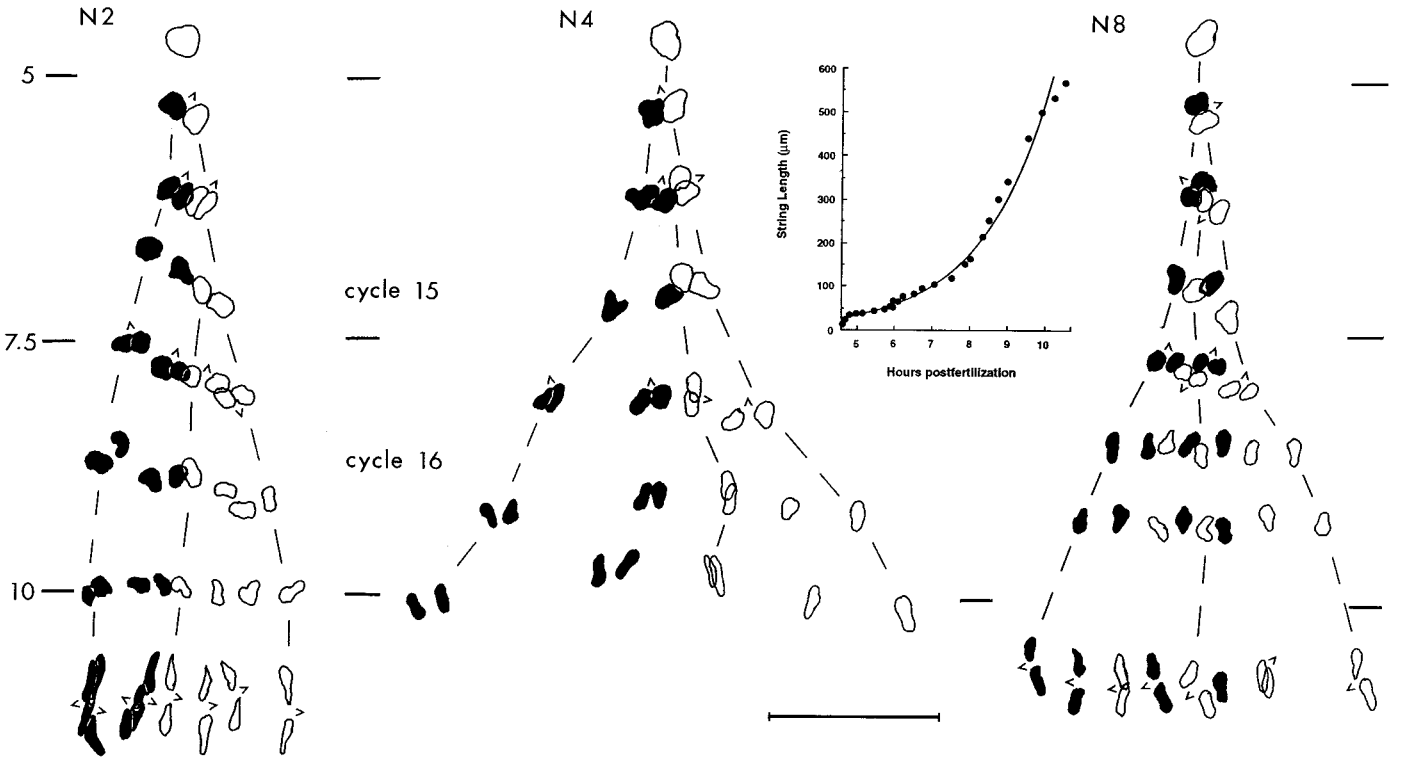


**Fig. 4.** Strings extend to variable lengths during cycles 15 and 16. The presentation is as in Fig. 3, but for each clone only the extension component of the morphogenetic movements of a cycle-13 deep cell sublineage is shown; epiboly and convergence are ignored. The sublineages later made hindbrain or, in the case of N4, hindbrain and rostral spinal cord (see Fig. 1). N2 was the most compact clone in our data set, and N4 was one of the more extended; this feature of a clone's morphology is due to the number of cell intercalation events that occur during cycles 15 and 16. Shading of anterior cells is for clarity; actually all of the cells contained the same tracer dye. In N8, mediolateral intercalations (movements oriented vertically in the figure) intersperse initially anterior (shaded) and posterior (white) cells along the string during both cycles 15 and 16. For N2 and N8, the figure shows the division ending cycle 16, and the subsequent bilateral splitting apart at the midline of the CNS primordium of the cycle 17 sister pairs. The inset shows the rate of string extension in the N4 sublineage, determined by measuring the distances between the most anterior and posterior cells in the string from video images, and fit to an exponential curve (the regression coefficient is 0.97). Curves for the other clones are similar but rise more slowly (not shown). Scale bar, 200 μm.

hollows into a neural tube; the neurocoele would probably block cell passage across the midline.

### Early neurons are born before morphogenesis ends

Division 16, the division that produces the bilateral sister pairs, is also the first birthday division of some neurons. A birthday division is one that generates at least one, and sometimes a pair of postmitotic differentiating cells (Fig. 7). Occasionally, bilateral homologues are sister cells (Table 2). The first neurons arise a cycle later than the first postmitotic notochord or muscle cells. We identified the neurons generated at division 16 as being 'primary' neurons (see legend to Fig. 7). Postmitotic 'secondary' neurons begin to be generated at division 17 and, in one clone, we observed a secondary motoneuronal birthday at division 18; usually our time-lapse recordings were not continued so long as in this case.

Hartenstein (1989) also reported that primary neurons are generated a cycle or more earlier than secondary neurons in the *Xenopus* neurula. Moreover, he described a tendency for sister cells to either both form primary neurons together, or both divide together and then form secondary ones. Sister cells in zebrafish sometimes become postmitotic together and make neurons of the same class (e.g. the c neuron pairs in N5 and N6; Fig. 7). However, in other examples, one sister becomes postmitotic and the other divides again (e.g. N3, N6). The detailed lineage relationships of particular kinds of neurons also appears variable, as illustrated in Fig. 7 by the several patterns of generation of the type c motoneurons.

## DISCUSSION

We have followed cell lineages in single clones during the late blastula, gastrula and early segmentation periods of zebrafish embryogenesis. We observed regular patterning in when cells divide, how they orient specific divisions and how they move and rearrange during interphases of specific cell cycles. Single clones generate long and narrow AP-oriented cell strings, first single and then, specifically for the CNS, bilaterally paired.

### Lineage may not determine fate

Clonal restriction might mean that cells inherit developmental commitments, but this seems unlikely for the early zebrafish embryo. Early gastrula cells are tissue-restricted (Warga and Kimmel, 1990), but they are not committed to their normal fates, as revealed by transplanting them as single cells to a new

blastoderm position (Ho and Kimmel, 1993). We show here that restriction to the CNS arises variably over several cell cycles, suggesting that it is not due to a singular patterning event. We also observed variability in lineage relationships of specific kinds of neurons, unexpected if lineage were determining neuronal identity. Transplanting young neurons after their final cell division can switch their fates, suggesting that position, not lineage, is the critical determinant of neuronal fate (Eisen, 1990).

Morphogenesis, in particular the formation of clonal strings, can account for tissue restriction. As gastrulation ends, the primordia of the axial organs are elongated cell fields, oriented, like a clonal string, along the AP-axis. This is clear considering the organization of the early fate map (Kimmel et al., 1990) and subsequent convergence and extension. Narrowing of the CNS primordium during gastrulation has been followed directly (Schmitz et al., 1993). Since a string is narrower and shorter than a primordium (e.g. the neural plate), and is oriented the same way, it is likely that usually a string will be contained within only one primordium and hence will develop only a single fate.

This idea would predict that occasionally a string would cross a primordium's A or P boundary, and make two different fates. Accordingly, we observed that, in single clones making both CNS and mesoderm, the anterior part of the cell string makes CNS and the posterior part makes mesoderm. This posterior part is closer to the zone of involution in the gastrula (Warga and Kimmel, 1990) and is captured by involution. The string folds back upon itself: the anterior part stays in an outer ectodermal primordium and the original posterior part folds into an underlying mesodermal primordium.

### Divisions and intercalations are coordinated

Cell intercalations during interphases, alternating with mitotic divisions, generate the clonal strings. Subtle differences in orientations of these events could result in either equal spacings between sisters and cousins (Fig. 8A) or greater spacings between cousins than between sisters (Fig. 8B); we observed both patterns (Fig. 4). We observed extension of strings after convergence to the midline is over, as could be brought about by continuing waves of convergence of lateral strings of cells upon and into the median one.

Strings lengthen at an exponential rate (inset, Fig. 4). These kinetics cannot be explained by exponential increase in cell number during gastrulation, for analysis of the data in Table 1 reveals that the cells are not growing exponentially. Rather, we propose that the exponential rate of string lengthening means that a combinatorial process is at work to make the strings. For example, imagine each single cell pulls a neighbor into its string at a rate that is constant. First, there would be 2 cells, then 4, then 8, and so on, until the period of string formation is over. Whatever the mechanism, evidently intercalation rates can vary among clones, for clonal strings are longer in the spinal cord than in the brain, and long strings, with their cells more dispersed, are produced by higher rates of intercalations during cycles 15 and

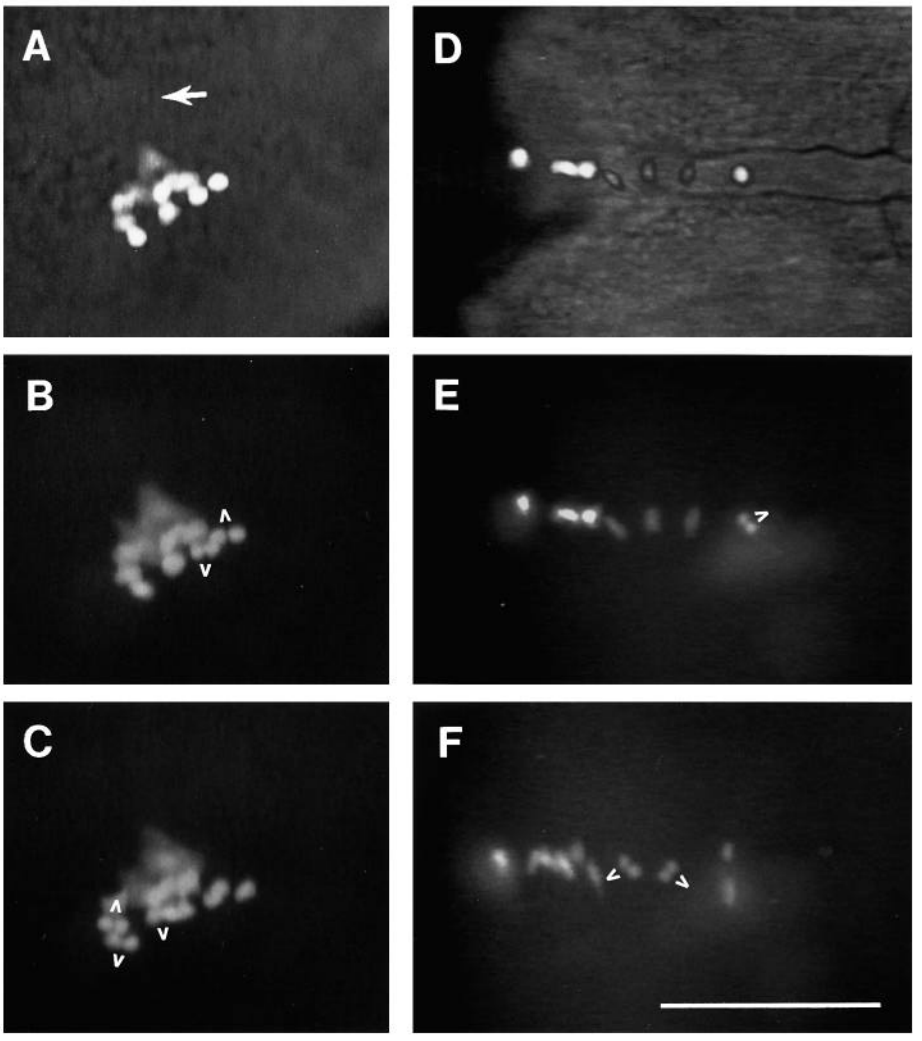


**Fig. 5.** Division 15 (A-C) frequently separates sister pairs longitudinally, and division 16 (D-F) frequently separates them transversely. Dorsal views with anterior to the left, from the video recordings of clone N2. The first panel in each set (A,D) combine bright-field and fluorescence to show the position of the clone relative the midline. In A (in the gastrula at 7.5 h), the cells, in interphase of cycle 15, have not reached the midline (at the arrow, as determined by the position of the notochord rudiment in the bright-field view). The 2 divisions (v) in B a minute later, and the 3 divisions in C 8 minutes later, are all in the transverse plane, separating sisters along the embryonic axis. D shows the clone exactly above the center of the notochord, just before the end of the interphase of cycle 16, at 10.7 h. The first division 16, a minute later (E), separates sisters to the left and right of the midline, and the other two, 3 minutes later (F) separate them obliquely. The cells continue to separate to the left and right subsequently. Scale bar, 200 μm.

**Table 2. Birthday divisions of particular cell types occur at particular cell cycles**

| Clone | Last division | Time (h) | Cell type |
|---|---|---|---|
| N* | 15 | 8:15 | Notochord, sister pair |
| N** | 15 | 8:46 | Notochord, sister pair |
| N10 | 15 | 9:00 | Somitic muscle, sister pair |
| N* | 16 | 9:40 | Spinal CaP primary motoneuron, bilateral sister pair |
| N6 | 16 | 10:12 | Spinal CaP primary motoneuron |
| N3 | 16 | 11:38 | Spinal ventral interneuron, ascending axon |
| N3 | 16 | 11:43 | Spinal MiP primary motoneuron |
| N4 | 16 | 12:23 | Spinal ventral interneuron, ascending axon |
| N10 | 16 | 13:43 | Somitic muscle, sister pair |
| N10 | 16 | 14:18 | Somitic muscle, two sister pairs |
| N11 | 16 | 14:35 | Dorsal root ganglion neuron, sister pair |
| N5 | 17 | 13:16 | Spinal type r secondary motoneuron |
| N3 | 17 | 14:32 | Spinal type c secondary motoneuron |
| N5 | 17 | 14:43 | Spinal type c secondary motoneuron, bilateral sister pair |
| N3 | 17 | 14:47 | Spinal type r secondary motoneuron |
| N6 | 17 | 15:44 | Spinal type c secondary motoneuron, sister pair |
| N2 | 17 | 17.19 | Cranial motoneuron, nerve VI (“m” in Fig. 1) |
| N5 | 18 | 21:27 | Spinal type r secondary motoneuron |

All of the clones except N* and N** are shown in Fig. 2. These two clones were not included there because of ambiguities in the lineages. Motoneuronal types are defined in the legend to Fig. 7.

16. Intercalation rate might vary according to AP position in the embryo, and could be important for patterning along the AP axis.

We observed unique morphogenetic behavior of CNS progenitors at the dorsal midline. Division 16, and subsequent cell movement reorient to separate sisters to the left and right. This patterning clearly differs from that in the *Xenopus* head and trunk, where many clones are restricted to one side or the other of the CNS (Jacobson, 1983). Taking the fate map of the CNS into account (Kimmel et al., 1990), we propose that this later-alwards *divergent* movement of sister cells is underneath, not into, the stream of cells still converging medially, and that such inward movement (Fig. 8C) is important for forming the neural tube. Cells near the dorsal midline early would form the bottom of the stack - the ventral parts of the neural tube. Cells that arrive at the midline later would divide and dive later, and consequently form the more dorsal parts of the neural tube. Our proposal would explain the progressive thickening of the neural anlagen, as well as its dorsoventral organization. Recently, Papan and Campos-Ortega (1994) have provided direct evidence for the proposal: they produced a fate map of the zebrafish neural plate and show that mediolateral cell arrangement in the plate corresponds to later dorsoventral arrangement in the tube. They also have independently found that cell divisions occur just in the midline of the developing neural keel, as we describe.

## Control of morphogenesis may drive cell lineage patterning

We did not expect, from previous work on early vertebrate development, to find cell cycle lengths increasing so uniformly in gastrulating cells and that distinguishable morphogenetic behaviors would occur at particular cell cycles. It is possible that regulation of cycle behaviors and morphogenetic cellular behaviors are interrelated. Altering by mutation the cell cycle at which a particular cell migration occurs in the *Caenorhabditis elegans* embryo disrupts subsequent morphogenesis (Nishiwaki et al., 1993).

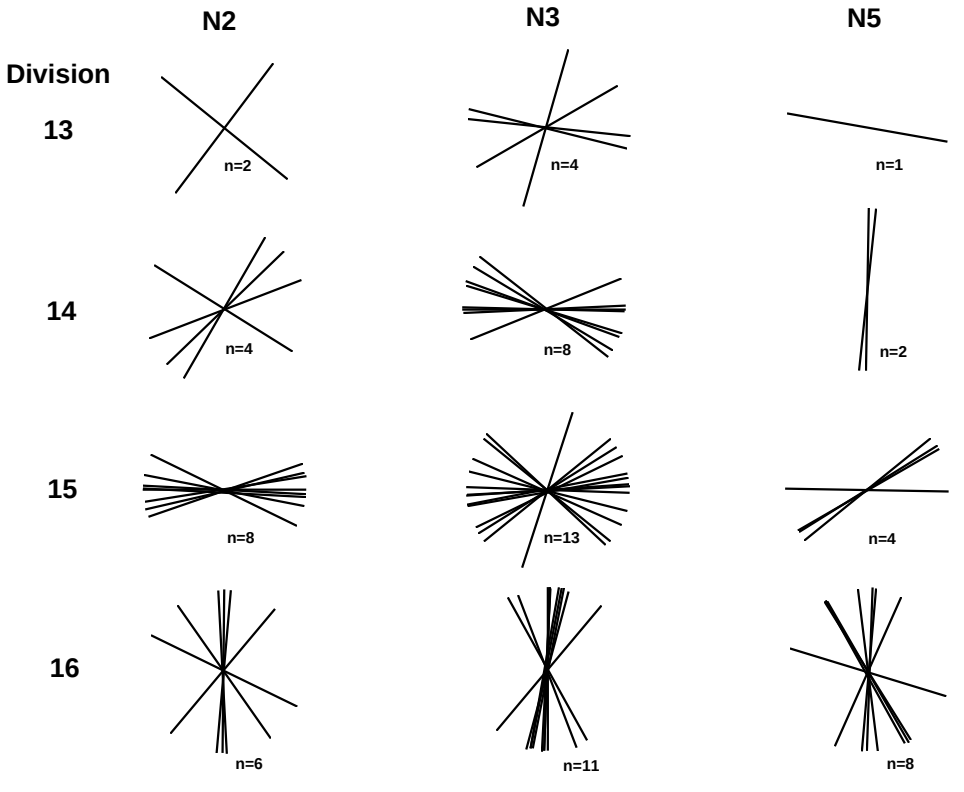


**Fig. 6.** Cell divisions become oriented by division 15 and the orientation changes at division 16 in clones N2, N3 and N5. Each line indicates the direction of separation of sisters immediately after a division. A horizontal line indicates a separation along the AP axis, and vertical line indicates a separation at a right angle to the axis, matching the orientations of the other figures. All but one or two of these divisions (n=71), irrespective of cycle number, were tangential (periclinal); producing sister cells in the same plane of focus as viewed from above the embryo. These three embryos were selected for this analysis because they were oriented almost exactly dorsal-up (e.g. Fig. 6D) during the recording, allowing unambiguous determination of the division planes.

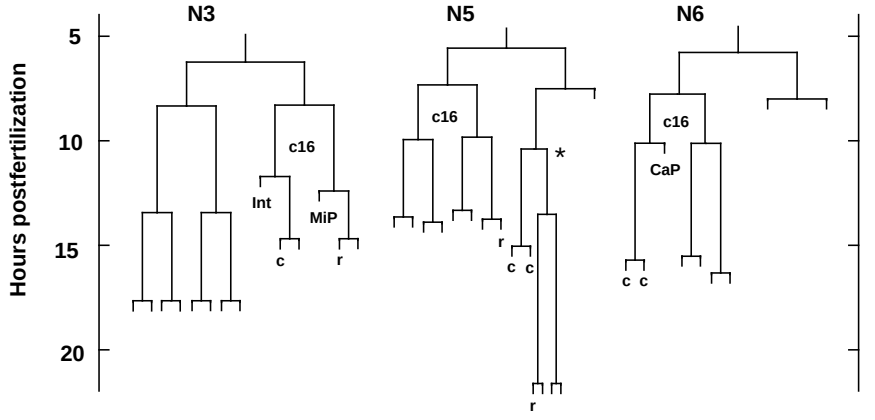


**Fig. 7.** Cycles 16-18 are the final cell cycles of some neurons. Particular sublineages are shown for three clones that generated motoneurons. The branches ending with postmitotic cells are indicated by letters designating the neuronal type, as determined by axonal morphologies, at 24 h and sometimes confirmed at later stages. By 24 h most primary neurons have grown long axons, but most secondary neurons have not (review: Kimmel and Westerfield, 1990). Primary neurons eventually grow larger and have the longest axons, and primary motoneurons in the spinal cord were previously known from [$^3$H]thymidine birthdating analysis to be generated earlier than secondary motoneurons in zebrafish (Myers et al., 1986). CaP and MiP (also RoP) are primary motoneurons, c and r indicate secondary motoneurons with CaP and RoP-like morphologies, and Int is a ventrally positioned primary interneuron with an ascending, ipsilateral axon in spinal cord. The positions of the cells are shown in Fig. 1, and the same sublineages can be located in Fig. 2, where the postmitotic cells are indicated by dots. The star at division 16 for clone N5 can be located in Fig. 2, and corresponds to the one in Fig. 3.

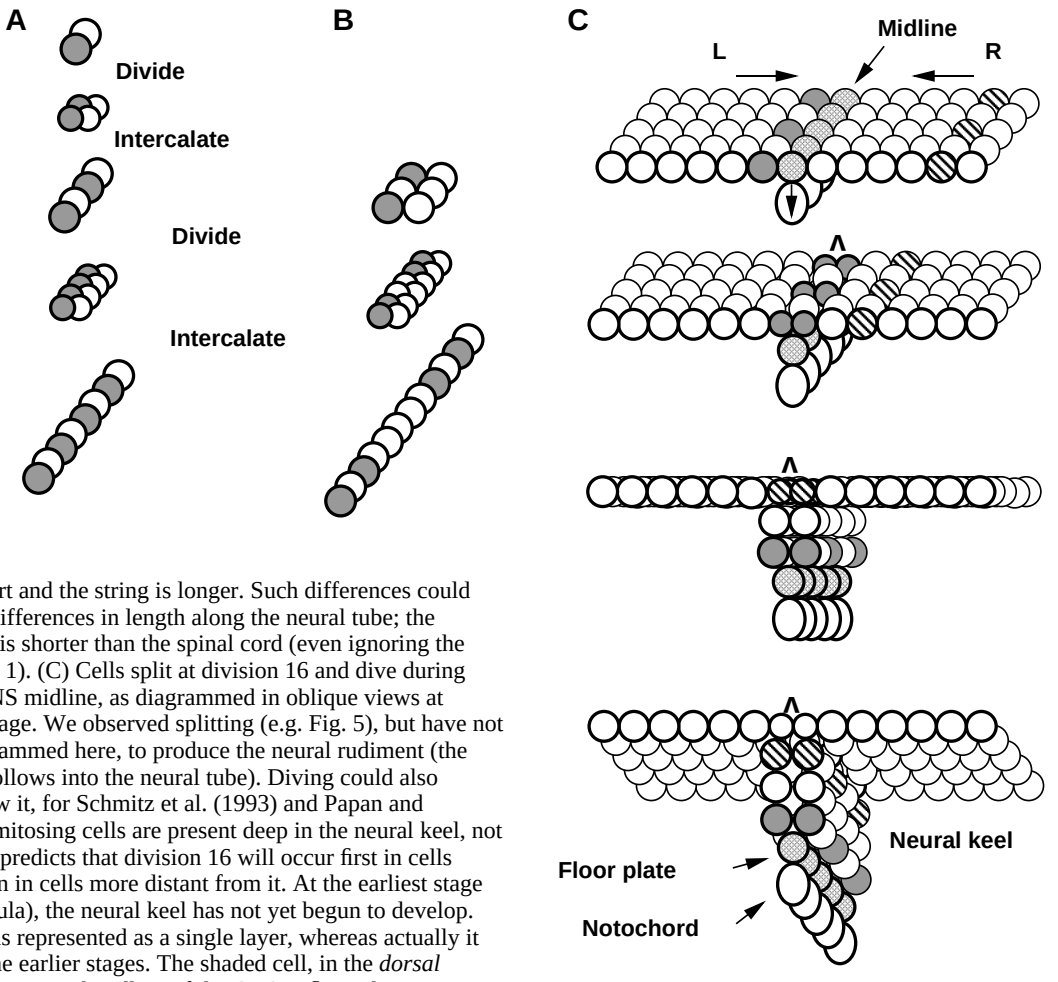


**Fig. 8.** Different oriented divisions and movements occur at different cell cycles. (A,B) Diagrammatic schemes in which oriented divisions 14 and 15 alternate with oriented intercalations during interphases 15 and 16 to produce strings with periodic (Warga and Kimmel, 1986) clonal distributions. At least two different regular patterns can arise by differences in these orientations. The distribution in A is like those observed in sublineages in N5 (Fig. 3), N2 and N8 (Fig. 4). The distribution in B is like that observed of the N4 sublineage in Fig. 4. More cells are involved in B than A, the labeled cells spread farther apart and the string is longer. Such differences could underlie, at least in part, regional differences in length along the neural tube; the hindbrain, where strings are short, is shorter than the spinal cord (even ignoring the tail), where strings are longer (Fig. 1). (C) Cells split at division 16 and dive during interphase 17 at the developing CNS midline, as diagrammed in oblique views at successive times going down the page. We observed splitting (e.g. Fig. 5), but have not verified that diving occurs as diagrammed here, to produce the neural rudiment (the neural keel, which subsequently hollows into the neural tube). Diving could also precede the cell division, not follow it, for Schmitz et al. (1993) and Papan and Campos-Ortega (1994) show that mitosing cells are present deep in the neural keel, not only in its dorsal parts. The model predicts that division 16 will occur first in cells originally closer to the midline than in cells more distant from it. At the earliest stage (upper diagram: early- to midgastrula), the neural keel has not yet begun to develop. The epiblast (primitive ectoderm) is represented as a single layer, whereas actually it could be multilayered, at least at the earlier stages. The shaded cell, in the *dorsal* midline of the epiblast will form the *ventral* midline of the CNS, a floor plate cell. Lateral cells, to the left (L) and right (R), are converging medially; the hatched cell string is farther from the midline than the stippled one. In the next view, the stippled cell string reaches the midline and the cells divide. Next, the sisters separate laterally and ventrally to the still converging epiblast cells. The hatched cell string reaches the midline and divides. Cells originating dorsomedially in the gastrula end up ventrally in the keel. This relocation is in accordance with the fate map (Kimmel et al., 1990; Papan and Campos-Ortega, 1994). Sisters are bilaterally paired along the wall of the neural keel, except for the floor plate cell, which does not seem to join the others in bilateral pairing, but forms a one-cell-wide median row (Hatta et al., 1991).

The controlling mechanisms that ensure proper morphogenesis seem to underlie the cell lineage patterning that we have observed. Clonal strings serve to record the history of expansion of an axial organ primordium by cell division, and also its regulated shaping - its narrowing and lengthening by convergence and extension. Moreover, as just discussed, bilateral symmetry in CNS clones seems to be revealing an unexpectedly precise cellular mechanism underlying neural tube formation, perhaps important for its bilateral shaping.

In support of this argument, we note that the bilateral dispersive movements that typically follow division 16 are the last large-scale movements separating cells from their neighbors to occur during development of the spinal cord. The first postmitotic young neurons are generated by the same division.

### How is patterning controlled?

The relationship between orientation of division and orientation of subsequent intercalations and movement is probably not a cause-effect one, as suggested by the behaviors of cells that do not follow the general trend. Pressure on the cells could be orienting their mitoses, hence their division planes. For example, during cycle 15, convergence, whatever its cause, might squeeze cells mediolaterally, to which they would respond by orienting the spindle longitudinally. Then, reaching the midline during cycle 16, we observe (unpublished) the cells to become elongated mediolaterally, as if here they are squeezed anterioposteriorly. In response, the spindle now orients transversely.

To account for cell cycle-specific morphogenesis one might propose that cells somehow count cell cycles (Temple and Raff, 1986; Quinn and Nameroff, 1983) and behave accordingly. Alternatively, the correlation between cycle number and morphogenetic pattern could simply be due to synchrony. Late gastrula deep cells are rather uniformly within cycle 16 and, possibly coincidentally, it is during this specific cycle that they are undergoing rapid mediolateral intercalations. Transplanting cells heterochronically might reveal whether morphogenetic behavior is causally dependent on cycle number.

We agree with Keller et al. (1991; 1992b) and Shih and Keller (1992a,b) that cells must be constrained to intercalate selectively between medial or lateral pairs of neighbors and hence move in an oriented fashion during convergence. The basis of this selectivity may be genetic, since convergence of somite precursor cells is specifically and autonomously perturbed by the mutation *spadetail* (Ho and Kane, 1990). It would be interesting to learn if clones of somitic precursors in this mutant can extend normally and form strings, in spite of this pronounced defect in convergence.

We observed singular morphogenetic behavior at the midline of the CNS primordium. This finding suggests that cells somehow sense they are at the midline, but how they might recognize this is unknown. The *cyclops* mutation autonomously and specifically perturbs patterning at the CNS midline (Hatta et al., 1991; Hatta, 1992), and the *no tail* mutation autonomously blocks development of midline mesodermal cells that would normally form notochord (Halpern et al., 1993). Both mutations may provide useful tools for learning the genetic control of morphogenesis at the embryonic midline.

We thank Ray Keller, Jay Mittenthal and many colleagues at the University of Oregon for criticizing drafts of the manuscript. Jose Campos-Ortega very graciously shared important manuscripts from his laboratory with us before their publication. Shawn Lockery helped with data analysis and Reida Kimmel provided technical assistance. Supported by NSF grant BNS 9009544 and NIH grants 5 T32 GM07412 10 and HD22486.

## REFERENCES

**Eisen, J. S.** (1990). Determination of primary motoneuron identity in developing zebrafish embryos. *Science* **252**, 569-572.

**Halpern, M. E., Ho, R. K., Walker, C. and Kimmel, C. B.** (1993). Induction of muscle pioneers and floor plate is distinguished by the zebrafish *no tail* mutation. *Cell* **75,** 1-20.

**Hartenstein, V.** (1989). Early neurogenesis in *Xenopus*: the spatio-temporal pattern of proliferation and cell lineages in the embryonic spinal cord. *Neuron* **3**, 399-411.

**Hatta, K.** (1992). Role of the floor plate in axonal patterning in the zebrafish CNS. *Neuron* **9**, 629-642.

**Hatta, K., Kimmel, C. B., Ho, R. K. and Walker, C.** (1991). The cyclops mutation blocks specification of the floor plate of the zebrafish CNS. *Nature* **350**, 339-341.

**Ho, R.K. and Kane, D.A.** (1990). Cell-autonomous action of zebrafish *spt-1* mutation in specific mesodermal precursors. *Nature* **348**, 728-730.

**Ho, R. K. and Kimmel, C. B.** (1993). Commitment of cell fate in the early zebrafish embryo. *Science* **261**, 109-111.

**Jacobson, M.** (1983). Clonal organization of the central nervous system of the frog. III. Clones stemming from individual blastomeres of the 128-, 256-, and 512-cell stages. *J. Neurosci.* **3,** 1019-1038.

**Kane, D. A. and Kimmel, C. B.** (1993). The zebrafish midblastula transition. *Development* **119**, 447-456.

**Kane, D. A., Warga, R. A. and Kimmel, C.B.** (1992). Mitotic domains in the early embryo of the zebrafish. *Nature* **360**, 735-737.

**Keller R., Shih, J. and Sater, A.** (1992a). The cellular basis of the convergence and extension of the *Xenopus* neural plate. *Dev. Dynam.* **193**, 199-217.

**Keller, R. E., Shih, J. and Domingo, C.** (1992b). The patterning and functioning of protrusive activity during convergence and extension of the *Xenopus* organizer. *Development* **1992 Supplement**, 81-91.

**Keller, R. E., Shih, J. and Wilson, P. A.** (1989). Morphological polarity of intercalating deep mesodermal cells in the organiser of *Xenopus laevis* gastrulae. *Proc. 47th Ann. Electron Microscop. Soc. Am.*, p. 840, San Francisco Press.

**Keller, R., Shih, J., Wilson, P. A. and Sater, A. K.** (1991). Patterns of cell motility, cell interactions, and mechanism during convergent extension in *Xenopus*. In *Cell-Cell Interactions in Early Development.* (ed. G. C. Gerhart), *Soc. Devel. Biol, 49th Symp.*, pp. 31-62.

**Keller, R. E. and Tibbetts, P.** (1989). Mediolateral cell intercalation is a property of the dorsal, axial mesoderm of *Xenopus laevis*. *Dev. Biol.* **131**, 539-549.

**Kimmel, C. B. and Warga, R.** (1986). Tissue specific cell lineages originate in the gastrula of the zebrafish. *Science* **231**, 365-368.

**Kimmel, C. B. and Warga, R. M.** (1987). Cell lineages generating axial muscle in the zebrafish embryo. *Nature* **234**, 234-237.

**Kimmel, C.B., Warga, R. M. and Schilling, T.F.** (1990). Origin and organization of the zebrafish fate map. *Development* **108**, 581-594.

**Kimmel, C. B. and Westerfield, M.** (1990). Primary neurons of the zebrafish. In *Signals and Sense: Local and Global Order in Perceptual Maps*, (ed. G. M. Edelman, W. E. Gall, and W. M. Cowan), pp 561-588, New York: John Wiley & Sons.

**Myers, P. Z. and Bastiani, M. J.** (1991). Neurovideo: a program for capturing and processing time-lapse video. *Comp. Meth. Prog. Biomed.* **34**, 27-33.

**Myers, P. Z., Eisen, J. S. and Westerfield, M.** (1986). Development and axonal outgrowth of identified motoneurons in the zebrafish. *J. Neurosci.* **6**, 2278-2289.

**Nishiwaki, K., Sano, T. and Miwa, J.** (1993). *emb-5*, a gene required for the correct timing of gut precursor cell division during gastrulation in *Caenorhabditis elegans*, encodes a protein similar to the yeast nuclear protein SPT6. *Mol. Gen. Genet.* **239,** 313-322.

**Papan, C. and Campos-Ortega.** (1994). On the formation of the neural keel and neural tube in the zebrafish, *Brachydanio rerio. Roux's. Arch. Dev. Biol.*, in press.

**Quinn, L. S. and Nameroff, M.** (1983). Analysis of the myogenic lineage in

chick embryos. III. Quantitative evidence for discrete compartments of precursor cells. *Differentiation* **24**, 111-123.

**Schmitz, B., Papan, C. and Campos-Ortega, J. A.** (1993). Neurulation in the anterior trunk region of the zebrafish *Brachydanio rerio. Roux's. Arch. Dev. Biol*. **202,** 250-259.

**Schoenwolf, G. C. and Alverez, I. S.** (1989). Roles of neuroepithelial cell rearrangement and division in shaping of the avian neural plate. *Development* **106**, 427-439.

**Schoenwolf, G. C. and Smith, J. L.** (1990). Mechanisms of neurulation: traditional viewpoint and recent advances. *Development* **109,** 243-270.

**Shih, J. and Keller, R.** (1992a). Cell motility driving mediolateral intercalation in explants of *Xenopus laevis*. *Development* **116**, 901-914.

**Shih, J. and Keller, R.** (1992b). Patterns of cell motility in the organizer and dorsal mesoderm of *Xenopus laevis*. *Development* **116**, 915-930.

**Streisinger, G., Singer, F., Walker, C., Knauber, D. and Dower, N.** (1986). Segregation analyses and gene-centromere distances in zebrafish. *Genetics* **112**, 311-319.

**Temple, S. and Raff, M. C.** (1986). Clonal analysis of oligodendrocyte development in culture: evidence for a developmental clock that counts cell divisions. *Cell* **44**, 773-779.

**Warga, R. M. and Kimmel, C. B.** (1990). Cell movements during epiboly and gastrulation in zebrafish. *Development* **108**, 569-580.

**Wilson, E. T., Helde, K. A. and Grunwald, D. J.** (1993). Something's fishy here--rethinking cell movements and cell fate in the zebrafish embryo. *Trends Genet.* **9**, 348-352.

(Accepted 8 November 1993)